

DESIGN IMPLICATIONS FOR EARTHQUAKE DURATION ON CONCRETE BRIDGE COLUMNS

David Sanders, PhD¹, Mohammed Saeed Mohammed, PhD²,
S. Mojtaba Alian³, Mohamed Moustafa, PhD³

Iowa State University¹, Dynamic Isolation System², University of Nevada, Reno³
Ames, Iowa¹; Reno, Nevada^{2,3}, United States

Abstract

Current bridge design methodologies do not take into account the impact of earthquake duration. This paper describes the performance of seismically designed reinforced concrete bridge columns under long-duration earthquakes. A previous experimental program, sponsored by the United States Federal Highway Administration (FHWA), included five identical columns that were tested on a shake table using long-duration motions from the Tohoku Earthquake. Responses were compared to a previously tested identical column that was subjected to a short-duration motion. Columns subjected to long-duration motions had substantially reduced displacement capacity. Phase II of the project, sponsored by the Pacific Earthquake Engineering Research Center (PEER), is developing ways to mitigate long-duration effects on concrete columns through detailing and specific design recommendations. The paper will describe the preliminary analysis on the mitigation strategies that will be investigated experimentally on a shake table.

Introduction

Long-duration earthquakes in Chile in 2010, 2014 and 2015, Japan in 2011, China in 2008, and Indonesia in 2004 have shown the impact of long-duration earthquakes. In addition, in areas such as Pacific Northwest of the United States, the Cascadia subduction zone has the potential to produce long duration earthquakes. Most seismic design specifications do not consider duration effects. Therefore a study was undertaken by Mohammed et al. (2017), funded by the Federal Highway Administration (FHWA), to study the impact of different types of earthquake, both long-duration and short-duration on five identical columns. As an extension of this project, the Pacific Earthquake Engineering Research Center (PEER) has funded a project that will test four more columns to investigate ways to mitigate the impact of long duration earthquakes and their impact on high strength reinforcement.

Base Specimen and Test Setup. The test specimens and setup used for both studies was adopted from Phan et al. (2005). The columns were 1/3-scaled bridge column. The original column was tested using the Rinaldi ground motion until failure. The height of each column was 72 in.; the diameter was 16 in.; the longitudinal reinforcement was 22 #4 bars; the transverse reinforcement was a 0.25-in. steel wire spiral with a 1.25 in. pitch; the axial load ratio was 8% of the column axial capacity; and the clear cover was 0.75 in. Specimen details and dimensions are shown in Fig. 1a. All columns were and will be tested on a shake table in the Earthquake Engineering Laboratory at the University of Nevada, Reno using the mass rig. The mass rig has been used extensively and allows the separation of the inertia mass from the axial load that is applied directly to the column using centerhold rams and Dywidag bars, see Fig. 1b. The ground motions are uniaxial. This paper will briefly discuss three of the five specimens tested in the FHWA project: LD-J1, LD-J2, and SD-L; and four specimens to be tested in the PEER project: LD-S3-G60, LD-S1.5-G60, LD-S1.5-G80, and LD-S1.5-G80D. LD stands for long-duration tests using earthquake records from Japan, while SD stands for one short-duration test that used a ground motion from the Loma Prieta earthquake. During the PEER project, changes will be made to the transverse and longitudinal reinforcement of the specimens. The original test by Phan et al. (2005) had maximum displacement of 9.8 in, which can be used for examining the impact of duration.

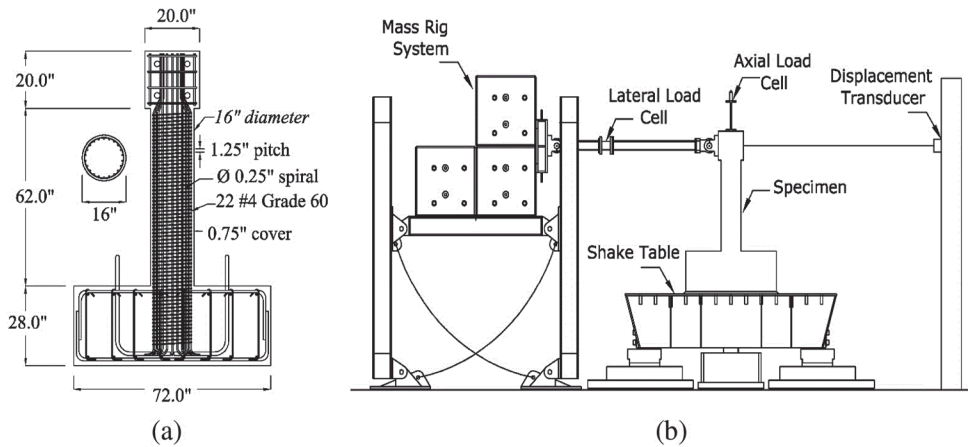


Figure 1. (a) FHWA project specimen details and dimensions (b) Test setup (Mohammed et al. 2017).

Phase I: FHWA Project

Ground Motion Selection

Open System for Earthquake Engineering Simulation (OpenSees, 2000), finite element package was used to conduct a pre-test analysis to choose ground motions in which the displacement demands on the columns are around half of its displacement capacity (9.8 in.). The analytical model was calibrated using the results from Phan et al. (2005). Based on the calibrated model, two long duration motions from the Tohoku 2011 earthquake (FKSH20 N-S and MYG006 E-W) were chosen for the columns LD-J1 and LD-J2 respectively, with significant durations (5-95% of Arias Intensity) of 88 and 115 seconds respectively, and a short duration motion from the Loma Prieta 1989 earthquake (Bran 00) was chosen for the Column SD-L, with a significant duration (5-95% of Arias Intensity) of 9.0 seconds. The long and short duration motions, but MYG006 E-W, were modified to match the response spectrum of Crescent City. Since the two motions have a similar spectral shape, the only difference between the two motions was their durations. Fig. 2 shows the acceleration histories for Column LD-J1 and Column SD-L, before and after the spectral matching. The spectral matching was done for a period range from 0.5 to 3 seconds. Fig. 3 shows the acceleration history for Column LD-J2.

The time axes of the selected ground motions was compressed by a factor of 0.577 to take into account the scaling from the prototype to the model (1/3 scale). The final motions response spectra are shown in Fig. 4.

Loading Protocol

The framework for the loading protocol for all columns was the same; the protocol began with the 100% of the selected motions and follow by an aftershock. Then scales of the main motions were applied until failure (125%, 150%, ..., etc.). The applied aftershock was the same for both columns and was chosen from the Mw 7.1 earthquake that occurred in Japan one month after the Tohoku earthquake.

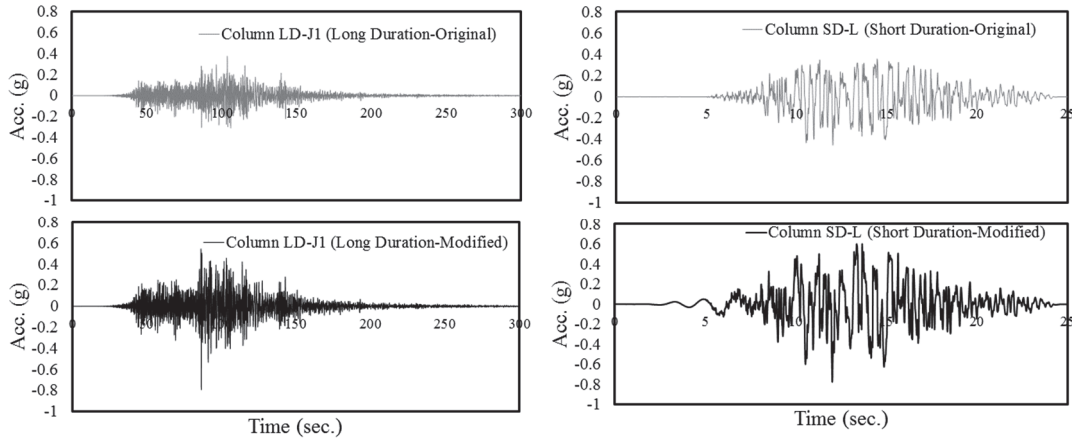


Figure 2. Acceleration histories for long and short-duration motions before and after spectral matching; Column LD-J1 (left set) and Column SD-L (right set) (Mohammed et al. 2017).

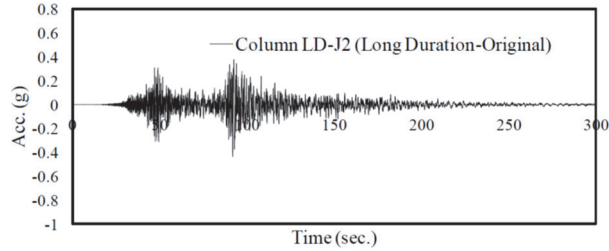


Figure 3. Acceleration history for the long-duration motion (Column LD-J2) (Mohammed et al. 2017).

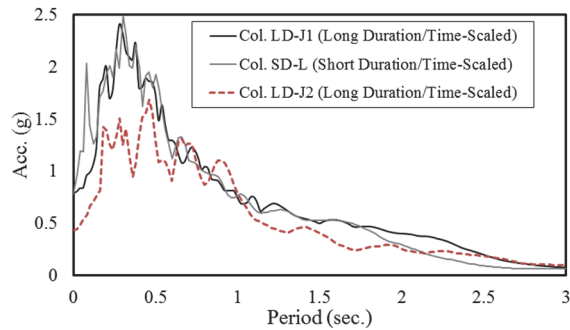


Figure 4. Response spectra of the final, time-scaled long and short-duration motions used in the FHWA project (5% damping) (Mohammed et al. 2017).

Test Results

Table 1 summarizes the damage states for the columns after each applied ground motion. The columns LD-J1 and LD-J2, which were subjected to the long duration motions, reached their final damage states after applying 125% of the main motions when four and one longitudinal bars fractured, respectively. The failure of the Column SD-L, with the short duration motion, did not occur until 175% of the main motion was applied and one bar fractured. Fig. 5 shows the damage states for the specimens after applying 125% of the main motion.

**Table 1. Comparison of the Actual Damage States between the Tested Columns
(Mohammed et al. 2017)**

Applied Motion	Actual Damage State		
	Column LD-J1	Column SD-L	Column LD-J2
100% of the main motion	-Max. Disp. = 4.5 in. -South: 4.4 in. spalling and the spirals are exposed. -North: 3.0 in. spalling and the spirals are exposed.	-Max. Disp. = 3.88 in. -South: cracks of max. width of 0.016 in. -North: 4.5 in. spalling and no exposed reinforcement.	-Max. Disp. = 4.7 in. -South: 7.5 in. spalling and the spirals are exposed. -North: 2.0 in. spalling and no exposed reinforcement.
Aftershock	-Same visual damage state as the previous motion.	-Same visual damage state as the previous motion.	-Same visual damage state as the previous motion.
125% of the main motion	-Max. Disp. = 4.98 in. -South: 8.5 in. spalling and four longitudinal bars fractured (failure). -North: 6.4 in. spalling and the concrete core is damaged.	-Max. Disp. = 4.8 in. -South: 4.5 in. spalling and the spirals are exposed. -North: 4.5 in. spalling and the spirals are exposed.	-Max. Disp. = 7.4 in. -South: 8.0 in. spalling and three longitudinal bars buckled. -North: 5.0 in. spalling and one longitudinal bar fractured (failure).
150% of the main motion	-Not applicable as bars fractured at 125% of the main motion.	-Max. Disp. = 7.3 in. -South: 9.0 in. spalling and the spirals are exposed. -North: 6.0 in. spalling and the spirals are exposed.	-Not applicable as fracture occurred at 125% of the main motion.
175% of the main motion	-Not applicable as bars fractured at 125% of the main motion.	-Max. Disp. = 9.2 in. -South: four longitudinal bars buckled. -North: one longitudinal bar fractured and two buckled.	-Not applicable as fracture occurred at 125% of the main motion.

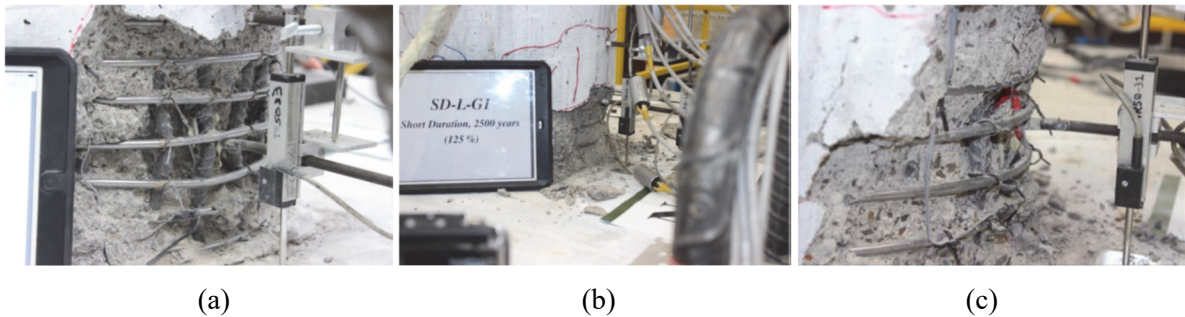


Figure 5. Damage states after applying 125% of the motion (a) Column LD-J1 (b) Column SD-L (c) Column LD-J2 (Mohammed et al. 2017).

The measured force-displacement hysteretic curves for the three specimens are shown in Fig. 6. The maximum displacement for Column LD-J1, Column SD-L, and Column LD-J2 were 4.98 in. (at 125% of the target motion), 9.2 in. (at 175% of the target motion), and 7.4 in. (at 125% of the target motion), respectively. The maximum displacement demands for Columns LD-J1 and LD-J2 were less than the displacement capacity, which was reached in Column SD-L test. Accordingly, the failure in LD-J1 and LD-J2 can be attributed to the large number of applied cycles, which indicates that long-duration motions can be more damaging than short-duration ones.

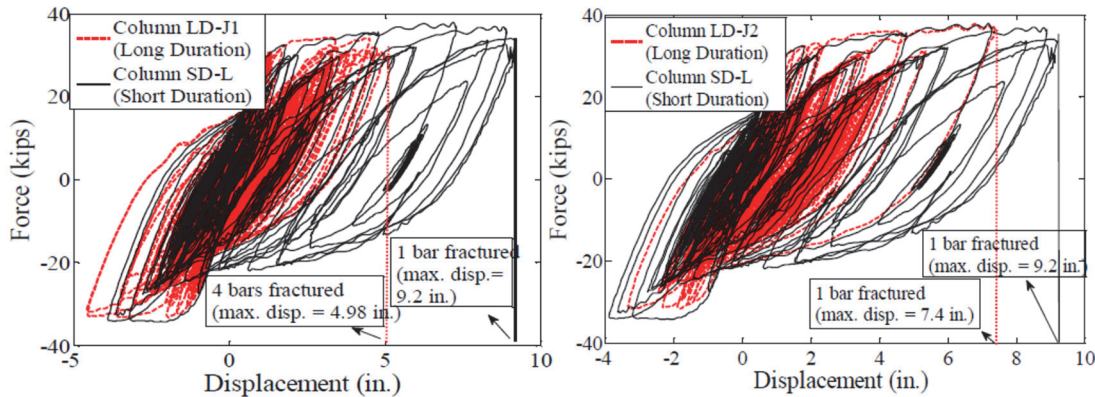


Figure 6. Comparison of the total cumulative force-displacement hysteretic curves (Columns LD-J1 and LD-J2 with Column SD-L) (Mohammed et al. 2017).

Phase II: PEER Project

Specimens Description

In phase II of the project, four 1/3-scale cast-in-place (CIP) bridge column models will be tested in two groups. The first group consists of two circular columns with similar geometry and longitudinal bars arrangement but different transverse reinforcement details than the FHWA project to investigate the effect of transverse bar spacing on the seismic performance of the columns. The longitudinal reinforcement will be 22 #4 bars (ASTM A706 Grade 60); and the transverse reinforcement will be a #3 bar with a 3 in. pitch for the first model, and a 1.5 in. pitch for the second model. The impact of long-duration earthquakes on high strength reinforcement will be investigated in the second test models group. Two circular columns reinforced longitudinally with ASTM A706 Grade 80 will be tested in the second group. The longitudinal reinforcement will be 18 #4 bars; and a #3 spiral with a 1.5 in. pitch will be used for the transverse reinforcement. Longitudinal bars in one of the columns in the second group will be debonded at the interface of the column and the footing. This is done to spread the bar yielding and to potentially overcome the low displacement capacity. Transverse reinforcement in all specimens will be ASTM A706 Grade 60. All columns are designed such that they have the same moment capacity. The details of the specimens are shown in table 2.

Table 2. Details of the Specimens in PEER Project

Specimen	LD-S3-G60	LD-S1.5-G60	LD-S1.5-G80	LD-S1.5-G80D
Diameter	16 in.	16 in.	16 in.	16 in.
Long. Reinf.	22 #4 (2.2%) Gr 60	22 #4 (2.2%) Gr 60	18 #4 (1.8%) Gr 80	18 #4 (1.8%) Gr 80
Trans. Reinf.	#3 @ 3 in. (1.04%)	#3 @ 1.5 in. (2.08%)	#3 @ 1.5 in. (2.08%)	#3 @ 1.5 in. (2.08%)
Long. Bars Clear Spacing	$6 d_b^\dagger$	$3 d_b$	$3 d_b$	$3 d_b$

[†] d_b : Longitudinal Bar Diameter

Analytical Modeling

OpenSees (McKenna, 2000) was used for pretest analytical studies. Fig. 7 shows a schematic view of the OpenSees model. The columns were modeled using nonlinear beam-column element with fiber section and expected material properties. A dead load of 80 kips resulting in an 8.0% axial load index was applied on the columns. The P-Delta effect was included in the analyses. Mass was lumped at the upper node of each column. Rotational inertial masses were not included. A damping ratio of 5% was used in dynamic analyses. The bond-slip effect at column-to-footing connection was modeled using the bond-slip model proposed by Wehbe et al. (1997) with a hysteretic tri-linear material assigned to a “zeroLength” element. The debonded bars were modeled using “trussSection” elements which were connected to the main element by “rigidLink” elements. In addition, to account for the failure of reinforcing bars due to low-cycle fatigue, the parent steel material assigned to the reinforcing bars was wrapped by the “Fatigue” material developed in OpenSees. The fatigue-fracture model developed by Zhong and Deierlein (2017) was used to determine low-cycle fatigue parameters.

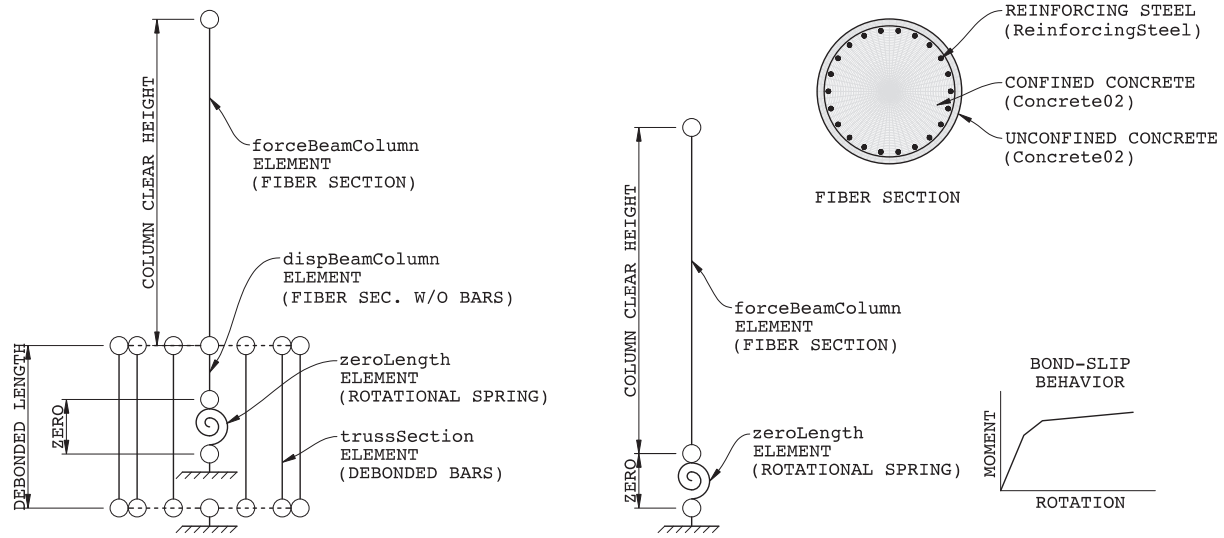


Figure 7. Schematic view of the OpenSees model for PEER project.

Loading Protocol

The loading protocol will be the same as the one used for the column LD-J2. All four columns will be subjected to 100% of the original record of 2011 Tohoku earthquake recorded at MYG006 E-W station then followed by an aftershock that occurred one month after the main earthquake. The main motion will be then incrementally amplified until failure (125%, 150%, ..., and so on).

Pre-Test Analysis

After the OpenSees model was calibrated with previous experimental results, four models were developed for the specimens. Nonlinear static analysis (Pushover) was conducted to determine the dominant failure mode, the displacement capacity, and the initial stiffness that was used in calculating the fundamental period of the columns. The reinforcement fracture was the dominant mode of failure in the models. Table 3 shows the results of pushover analysis. The results show 20% reduction in the stiffness of Gr80 columns compared to Gr60 columns, which is attributed to the lower longitudinal steel ratio in Gr80 columns. Debonding the longitudinal bars of specimen LD-S1.5-G80D resulted in a 51% increase in the displacement ductility capacity of the column.

Table 3. Results of Pushover Analysis for PEER Columns

Specimen	Yield Disp.	Ultimate Disp.	Disp. Ductility	Plastic Moment	Effective Stiffness	Period
LD-S3-G60	0.72 in.	6.53 in.	9.05	185 kip/in	42.8 kip/in	0.44 s
LD-S1.5-G60	0.73 in.	6.74 in.	9.23	186 kip/in	42.5 kip/in	0.44 s
LD-S1.5-G80	0.90 in.	5.28 in.	5.85	182 kip/in	33.5 kip/in	0.49 s
LD-S1.5-G80D	0.83 in.	7.35 in.	8.82	170 kip/in	34.1 kip/in	0.49 s

Nonlinear dynamic response history analysis (RHA) under the loading protocol was conducted on the columns. Park and Ang (1985) damage index were used with experimental fragility curves to predict the seismic performance and damage states of the columns as summarized in Table 4. Results show that the first three specimens are predicted to fail during run 3, while the failure of the last specimen is expected to occur during run 4.

Table 4. Predicted Performance of the Test Columns

Specimen	Run 1 (100%)		Run 2 (aftershock)		Run 3 (125%)		Run 4 (150%)	
	DI [†]	DS [†]	DI	DS	DI	DS	DI	DS
LD-S3-G60	1.3	80% E.R. [‡]	1.5	90% E.R.	2.8	95% B.F.	Not applicable	
LD-S1.5-G60	1.3	80% E.R.	1.4	85% E.R.	2.7	90% B.F.	Not applicable	
LD-S1.5-G80	1.2	80% E.R.	1.4	85% E.R.	2.7	90% B.F.	Not applicable	
LD-S1.5-G80D	1.1	70% E.R.	1.2	75% E.R.	2.3	90% B.B.	>3	100% B.F.

[†] DI: Park and Ang Damage Index; DS: Estimated Damage State.

[‡] Minor Spalling (M.S.); Extensive Spalling (E.S.); Exposed Reinforcement (E.R.); Longitudinal Bar Buckling (B.B.); and Longitudinal Bar Fracture (B.F.)

Summary and Conclusions

Seismic performance of reinforced concrete bridge columns under long-duration earthquakes has been investigated. In phase I of the project, five identical columns were tested on a shake table using long-duration motions from the Tohoku Earthquake. Results showed substantially reduced displacement capacity compared to the base specimen under the short-duration motion. Phase II of the project will test four more columns to investigate ways to mitigate the impact of long duration earthquakes and will include columns with high strength longitudinal reinforcement. Pre-test analytical studies showed the use of Gr80 steel instead of Gr60 reduced the stiffness of columns by approximately 20%. Debonding the longitudinal bars in the column-footing interface resulted in a 51% increase in the displacement ductility capacity of the column.

Acknowledgements

The studies presented in this paper were funded by the Federal Highway Administration under Contract No. -DTFH61-07-C-00031 and the Pacific Earthquake Engineering Center. The conclusions and findings in this paper are those of the authors and do not necessarily represent the views of the funding agencies.

References

- McKenna, F., Fenves, G., and Scott, M., (2000). "Open System for Earthquake Engineering Simulation (OpenSees)", Berkeley, California: Pacific Earthquake Engineering Research Center.
- Mohammed, M.S., Sanders, D.H., Buckle, I.G. (2017). "Reinforced Concrete Bridge Columns Tested Under Long and Short Duration Ground Motions," *16th World Conference on Earthquake Engineering*, Santiago, Chile, January 9-13, 2017.
- Park, Y., and Ang., A. H. (1985). "Mechanistic seismic damage model for reinforced concrete." *Journal of Structural Engineering*, 111(4), 740-757.
- Phan, V., Saiidi, M. S., and Anderson, J. (2005). "Near fault (near field) ground motion effects on reinforced concrete bridge columns." *Technical Report No. CCEER-05-07*, Center for Civil Engineering Earthquake Research, University of Nevada Reno, Reno, NV.
- Wehbe, N., Saiidi, M., and Sanders, D. (1997). "Effects of Confinement and Flares on the Seismic Performance of Reinforced Concrete Bridge Columns", Civil Engineering Department, University of Nevada, Reno, CCEER 97-2, November 1997.
- Zhong, K., Deierlein, G. (2017). "Low-Cycle Fatigue Criteria for the Seismic Design of Concrete Structures with High Strength Reinforcing Steel", *Interim Report II*, CPF Research Project RGA #02-16, Charles Pankow Foundation.